



# Effect of Bone Marrow Mesenchymal Stem Cells on a Short-Term Induced Diabetic Retinopathy in Adult Female Albino Rats

Nahla Imbarak<sup>1,2</sup> · Horeya Erfan Korayem<sup>1</sup> · Nema Soliman<sup>1,2</sup> · Somaya Hosny<sup>1,2</sup>

Received: 15 May 2022 / Revised: 22 May 2023 / Accepted: 27 May 2023 / Published online: 17 July 2023  
© The Author(s), under exclusive licence to The Regenerative Engineering Society 2023

## Abstract

**Background** Worldwide, diabetic retinopathy (DR) remains the leading cause of visual impairment that often leads to irreversible vision loss. Despite the screening programs and treatments, DR affects approximately 17.9% of type II diabetes patients in Egypt.

**Aim** To assess the curative effect of intravitreally injected bone marrow mesenchymal stem cells on experimentally induced diabetic retinopathy.

**Methods** Thirty adult female albino rats were randomized into 5 groups: group (I), received no treatment; group (II), received intravitreal injection of phosphate buffer saline; group (III), subjected to diabetes induction using intraperitoneal injection of streptozotocin; group (IV), received intravitreal injection of bone marrow mesenchymal stem cells (BM-MSCs); and group (V), received intravitreal injection of BM-MSCs post-diabetes induction. After 30 days, the right eyes were enucleated and prepared for histological stains (H&E and PTAH), histochemical stain (PAS), and immunohistochemical stains (anti-CD34, anti-caspase-3 active, and anti-fibronectin), and the left eyes of group (V) were prepared for PCR analysis.

**Results** Group (V) revealed preserved retinal tissue integrity, and the cellular organization appeared nearly normal in comparison to control groups. Less gliosis was seen in group (V) in comparison to group (III). Morphometric analysis of group (V) revealed a statistically significant increase in retinal thickness and decrease of the optical density of CD34 and fibronectin immunoreaction compared to group (III). PCR results revealed that all recipient rats contain SRY-positive gene.

**Conclusion** BM-MSCs significantly reduced neurovascular retinal degeneration and gliosis within treated animals. BM-MSCs might be beneficial in preventing DR progression.

**Lay Summary** Diabetic retinopathy remains the leading cause of visual impairment which could progress up to visual loss. Vaso-regenerative stem cell therapy could be an effective therapeutic approach to prevent progression of retinal nerve cell damage in patients with ischemic retinopathies including diabetic retinopathy. In the present study, we investigated the therapeutic effect of intravitreally injected BM-MSCs in a short-term experimentally induced diabetic retinopathy. BM-MSCs could provide a partial curative effect on the retina through decreasing retinal nerve cell degeneration, microangiopathies, fibrosis, and gliosis.

Further studies focusing on the quality and timing of stem cell injection in different diabetic retinopathy stages and effectiveness of cell therapy as well as the possible adverse effects are recommended.

**Keywords** Animal model · Diabetic retinopathy · Diabetes complications · Stem cell transplantation

✉ Nahla Imbarak  
nahla\_mubarak@med.suez.edu.eg

Horeya Erfan Korayem  
horeya.arafat@med.suez.edu.eg

Nema Soliman  
nema.abu\_maziad@med.suez.edu.eg

Somaya Hosny  
Somaya@med.suez.edu.eg; Somaya@hotmail.com

<sup>1</sup> Department of Histology and Cell Biology, Faculty of Medicine, Suez Canal University, Ismailia 41522, Egypt

<sup>2</sup> Center of Excellence in Molecular and Cellular Medicine, Faculty of Medicine, Suez Canal University, Ismailia 41522, Egypt

## Introduction

Diabetic retinopathy (DR) is the primary cause of visual impairment in adults in developing countries. The prevalence of type II diabetes in adults, aged above 50 years, is approximately 20.9% in Egypt while estimated 34.6% worldwide. Diabetic retinopathy affects approximately 17.9% of type II diabetic patients in Egypt [1, 2].

Diabetic retinopathy is clinically categorized based on the presence of vascular lesions into an early-stage non-proliferative DR and a later stage proliferative DR. The non-proliferative stage is characterized by microvascular changes, dot and blot hemorrhages, microaneurysms, cotton wool spots, capillary non-perfusion, and exudates. The proliferative stage is characterized by the newly aberrant fragile vessels and macular edema [1].

Retina has remarkably high metabolic needs and continuous demand for oxygen and nutrients. Hence, two vascular beds nourish the retina. The outer retinal five layers are avascular and rely on an indirect supply from the choriocapillaris, while the inner retina receives direct blood supply from the central retinal artery and vein [3]. Retinal blood vessels' structure is like vessels elsewhere, except the absence of internal elastic lamina from the arteries, and muscle cells may be seen in the adventitia. Retinal capillaries are composed of non-fenestrated endothelial cells surrounded by supporting intramural pericytes, astrocytes, and Muller cells endfeet [4].

With the advancement in diagnostic tools, studies proved that alterations in the neuroretinal function are the earliest sign of DR in the experimental models. In the vascular component, pericytes are the first to die, followed by gradual capillary endothelial cell loss that leads to naked basement membrane tubes which cause ghosts appearance [3]. It is reported that pericyte death and consequent increase in vascular dysfunction resulted in capillary dilatation, permeability changes, and increased blood flow that occur as early as 8 days after the onset of diabetes in rats [5]. After 2 weeks, disturbance of the inner blood-retinal barrier and increase number of apoptotic cells were evidenced. However, Muller cells and microglial cells increased after 1 month of hyperglycemia [6]. The excessive increase of Muller cells is harmful, as they induce morphological and functional alterations from the early phases of the DR disease which lead to failure in regulating the retinal blood flow or maintaining the blood-retinal barrier [7].

After 2 months of hyperglycemia, neovascularization was observed, on the surface of the retina, and penetrates the inner limiting membrane into the vitreous [6, 8]. These new vessels are typically fenestrated, fragile, and leaky which can lead to vitreous hemorrhage. Repeated vitreous hemorrhage is associated with fibro-vascular scar formation [9].

Over a century of studies, researchers are still identifying all of the complexities of eye functions, mechanisms of disease progression, and new advances in blindness prevention [10]. Currently, there are still no accurate therapies or protective agents for diabetic retinopathy preventing changes in the retinal vasculature or halting the progression of DR and consequently preserve vision. Finding new modalities to prevent or restore visual function after severe retinal nerve cell damage through regenerative medicine is the next key frontier in ophthalmology.

Initial evidences, from preclinical studies, indicate that stem cell therapy could be an effective therapeutic option for diabetic retinopathy [8]. Bone marrow mesenchymal stem cells (BM-MSCs) are one of these modalities. BM-MSCs are multipotent stem cells that can differentiate into neural tissue; exert paracrine effects by secreting neurotrophic growth factors, like brain-derived neurotrophic factors, ciliary neurotrophic factor, and basic fibroblast growth factor; exhibit anti-inflammatory reaction; and promote angiogenesis by secreting different neurotrophic factors [10, 11]. BM-MSCs also secrete neurotrophic factors that have a neuroprotective and neurogenic effect to retinal neurons [12]. BM-MSCs are also well known to secrete a wide range of pro-regenerative, mitotic, anti-apoptotic, and anti-fibrotic factors. These factors modify the local microenvironment from an injury state to a pro-regenerative state [13].

It was reported that the integration of intravitreally injected BM-MSCs into the different retinal layers decreased the retinal gliosis after 3 months of the injection [14]. Wang et al. [15] found that intravitreal injection of human BM-MSCs increased remodeling and regeneration of injured vessels in diabetic retinopathy models (rats and mice) after 6 weeks of the injection. In addition, Xu et al. [16] highlighted on the anti-inflammatory and anti-apoptotic effects of microRNA 18b secreted from MSCs' extracellular vesicles in rats with DR.

Although several studies investigated the effect of stem cells on diabetic retinopathy in different animal models, using either histological, histochemical, and/or immunological techniques, in this study, we used all the previous techniques to get a more holistic view on the effect of intravitreally injected BM-MSCs in a short-term experimentally induced DR.

## Materials and Methods

### Experimental Design

Our study was carried out in the Center of Excellence in Molecular and Cellular Medicine, Faculty of Medicine, Suez Canal University, Egypt. After the approval of the

Institutional Research Ethics Committee (IORG0005275), thirty female Wistar albino rats, aged 6–7 months and weighing between 200 and 250 g, were used in this study. Additionally, 10 male albino rats, 4–6 weeks old and weighing around 150 g, were used for BM-MSC extraction (to obtain bone marrow rich in stem cells). Animals were brought from the National Research Center for Experimental Animals, Cairo. Animals were acclimatized to their place for 1 week before the start of the experiment and housed in their cages (one animal/cage) and fed with a high-fat diet.

Female rats were divided into five groups (6 animals/group): group I (control (1) group), animals did not receive any treatment; group II (control (2) group), each animal received an intraperitoneal injection of 35 mg/kg phosphate buffer saline (PBS) at day 1 and then received an intravitreal injection of 5  $\mu$ L PBS in each eye at day 11 [17]; group III (diabetic retinopathy group), each animal received an intraperitoneal injection of 35 mg/kg streptozotocin at day 1 [6]; group IV (mesenchymal stem cells group), each animal received an intraperitoneal injection of 35 mg/kg of PBS at day 1 and then received an intravitreal injection of  $2 \times 10^5$  BM-MSCs at day 11 [18]; and group V (diabetic retinopathy and mesenchymal stem cells group), each animal received an intraperitoneal injection of 35 mg/kg of streptozotocin, at day 1, followed by intravitreal injection of  $2 \times 10^5$  BM-MSCs at day 11 [11].

Body weight was recorded once weekly for each animal until the end of the experiment.

## Type II Diabetes Induction

At day 1 of the experiment, after overnight fasting, rats received a single dose of 35 mg/kg streptozotocin (STZ) from (Sigma, Egypt) dissolved in saline and injected intraperitoneally. After 72 h, animals were declared diabetic when their blood glucose exceeded 220 mg/dl for 3 consecutive days. Blood glucose level was recorded using OK Biotech Co., Ltd., Taiwan, kits once weekly after 4–5 h of fasting [6].

## Isolation and Culture of MSCs from Male Rats' Bone Marrow

In the tissue culture unit, under sterile conditions, bone marrow from femurs and tibias was flushed with low-glucose Dulbecco's modified Eagle medium supplemented with 10% fetal calf serum and 1% penicillin–streptomycin (Lonza Bioproducts, Belgium) from one end of the bone and received in a falcon tube from the other end [19]. The marrow was washed more than once with PBS (Lonza Bioproducts, Belgium) for 5 min at 2000 rpm [20]. Isolated cells were cultured to adjust a density of  $1 \times 10^6$  cells per well in full culture media. Cultures were kept at 37 °C in a humidified incubator with 5% CO<sub>2</sub>

and 95% air infusion. When cells reached ~90% confluence, cells were trypsinized with 0.25% trypsin containing 0.02% ethylene diamine tetra-acetate (EDTA) (Lonza Bioproducts, Belgium). The action of the trypsin/EDTA was then blocked by adding complete medium [21]. The cells were maintained in culture and expanded till passage three.

## Flow Cytometry

Immunophenotypic assessment of the BM-MSC surface markers was done in the third passage cultured cells. Ten microliters of specific IOTest conjugated antibodies (anti-CD105 and CD90) from eBioscience was added to the test tubes and 10  $\mu$ l of control was added to the control tube. After adding the test sample and mixing, the tubes were incubated for 20 min at 18–25 °C in the dark. The tubes were centrifuged for 5 min at 150  $\times$  g at room temperature. Cell pellets were resuspended in 0.5–1 ml of PBS in 2–8 °C in a dark room for up to 20 min and then centrifuged. Cell pellets were resuspended using 3 ml of PBS and were passed through a 70-mm filter and analyzed for surface marker profile by flow cytometry (CyFlow Space—Partec).

## Mesenchymal Stem Cell Administration

Before intravitreal injection, to ensure compliance with ethical considerations, rats were anaesthetized using intramuscular injection of 75 mg/kg ketamine (EPICO, Egypt) [22].

Mesenchymal stem cells were injected on day 11 from the start of the experiment. After anesthesia, the pupil of both eyes was dilated with tropicamide eye drops (Alcon, Egypt); then, a single dose of  $2 \times 10^5$  BM-MSCs suspended in 5  $\mu$ L PBS was injected gradually and slowly intravitreally using an appropriately sized needle in the supero-temporal part of the eye. The needle was introduced 2 mm posterior to the limbus [11]. A surgical microscope (Zeiss Stemi 2000) was used to observe the needle in the vitreous.

## Retinal Preparation

At the end of the experiment, at day 30, rats were sacrificed by an overdose of ketamine [23]. Right eyes were rapidly enucleated and fixed in Davidson's solution for 48 h and then placed in ethanol and processed for 6- $\mu$ m paraffin sections for histological (hematoxylin and eosin [H&E] and phosphotungstic acid-hematoxylin [PATH]), histochemical (periodic acid Schiff [PAS]), and immunohistochemical assessment (anti-CD34, anti-caspase-3 active, and anti-fibronectin). Left eyes were enucleated and the frontal sections and the lenses were removed under the surgical microscope; then, the posterior sections were frozen in –80 °C for PCR.

## Immunohistochemical Stains (for Retinal Vasculature, Cellular Apoptosis, and Fibrosis)

Sections were dewaxed and passaged in different alcohol concentrations and then washed with PBS. Endogenous peroxidase was blocked by 0.006% hydrogen peroxide drops for 10–20 min and washed by distilled water for 5 min. Fragment crystallizable (Fc) receptors were blocked by normal horse serum and were wiped around. Sections were incubated with primary rabbit anti-rat polyclonal anti-CD34 antibody at a dilution (1:100) [24], anti-caspase-3 active antibody at a dilution (1:2000) [25], and anti-fibronectin antibody at a dilution (1:100) [26] for 1 h at room temperature. After washing with PBS, sections were incubated with biotin-labeled 2<sup>ry</sup> antibody for 30 min at room temperature and then washed three times with PBS. Streptavidin–Horse-radish Peroxidase Conjugate dilution buffer was applied for 20–30 min at room temperature to enhance staining intensity. Sections were then washed with PBS and were incubated with diaminobenzidine chromogen for 5 min at room temperature and counterstained with hematoxylin for 30 s. After washing, sections were dehydrated through 95% ethanol and then 100% ethanol. Slides were mounted in DPX. To avoid inaccurate conclusions, positive and negative controls were run.

## Polymerase Chain Reaction

To identify male donor-derived cells in female recipients, posterior section of the left eyes from group V and, in addition, an eye from normal female and male rats was isolated to be used as negative and positive controls, respectively. PCR amplification of a part of the SRY gene, on chromosome Y: 327,166–329,299 (Ensembl: ENSRNOG00000062090), using a primer set with a size of 287 bp and with the following sequence: F5' primer, 5'-GGC TCA ACA GAA TCC CAG CA-3' and R3' primer 5'-TAG CCC AGT CCT GTC CGT AT-3' [27].

In the molecular biology unit, PCR reaction was performed in a thermal cycler (Veriti 96 Well, thermal cycler) at 95 °C for 2 min for initial denaturation followed by 45 cycles of 94 °C for 30 s for denaturation, 56 °C for 1 min for annealing, and 72 °C for 1 min for extension, with a final extension of the cycle at 72 °C for 5 min. Gel analysis was done using 4 µl of loading buffer (Qiagen, Germany) added to 10 µl of each PCR product, and then, they were loaded to the prepared gel (agarose gel 0.8 in 1 × TAE buffer), and the current was on for 45 min.

## Morphometric Measurements

To standardize the measurements, three sections/animal and five fields/section from the center of the retinas were

measured using computer-assisted image analysis Pro-Plus software that was calibrated before use. Using an objective lens of magnification (×400), ganglion cell count (GCC) [28] and the thicknesses of the outer nuclear layer (ONL), the inner nuclear layer (INL), the ganglion cell layers (GCL), and the nerve fiber layer (NFL) were measured [11]. The optical density of the CD34 immunostained endothelial cells [24] and the optical density of the fibronectin immunostained areas [26] were assessed. All measurements were chosen randomly with non-overlapping fields in each section.

## Statistical Analysis

Frequency distribution of the changes found was calculated for the four groups. Using the Statistical Package for Social Sciences (SPSS 22 software), results were expressed as mean ± SD, and  $P < 0.05$  was considered statistically significant. The statistical significance was determined by one-way analysis of variance (ANOVA) with Duncan post hoc test to compare the differences between groups.

## Results

### Animals' Weight

In the 1st week, there were no significant differences in body weight between control groups in comparison to DR group ( $P = 0.095$ ), MSCs group ( $P = 0.999$ ), and DR and MSCs group ( $P = 0.064$ ). In the 2nd, 3rd, and 4th week, there was a significant increase in body weight in the DR group and DR and MSCs group in comparison to control groups ( $P = 0.0001$ ). There was no significant difference in body weight between control groups in comparison to MSCs group in the 2nd, 3rd, and 4th week ( $P > 0.05$ ) (Fig. 1 and Table 1).

### Blood Glucose Level

At day 1, there were no significant differences between control groups in comparison to DR group ( $P = 0.774$ ), MSCs group ( $P = 0.918$ ), and DR and MSCs group ( $P = 0.297$ ). At day 4 and 2nd, 3rd, and 4th week, there was a significant increase in the blood glucose level in the DR group and DR and MSCs group in comparison to control groups ( $P = 0.001$ ). There was no significant difference between control groups in comparison to MSCs group at day 4 and 2nd week, 3rd week, and 4th week ( $P > 0.05$ ) (Fig. 2 and Table 2).

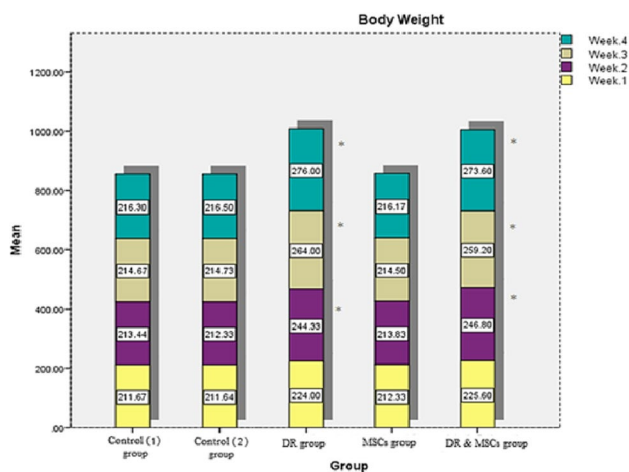


**Fig. 1** Comparison between mean body weight among different experimental groups in 1–4 weeks. \*significant difference ( $P=0.0001$ )

### Characterization of BM-MSCs

#### Morphological Assessment

Using inverted microscope (LEICA S 80/0.30), the adherent BM-MSCs appeared fusiform in shape, varied in size with central nuclei and cytoplasmic prolongations. They adhered to the tissue culture substrate within 72~96 h. They reached confluence within ~9 days in 50-ml tissue culture flask (Fig. 3).

#### Immunophenotypic Assessment

Cultured cells from passage three showed that 94.22% of cells are positive for both CD105 and CD90 surface markers (Fig. 4).

#### Histopathological Findings

##### Hematoxylin and Eosin (H&E) Stained Sections

Histological examination of retinal samples in groups I and II (control groups) showed normal structure. The retina

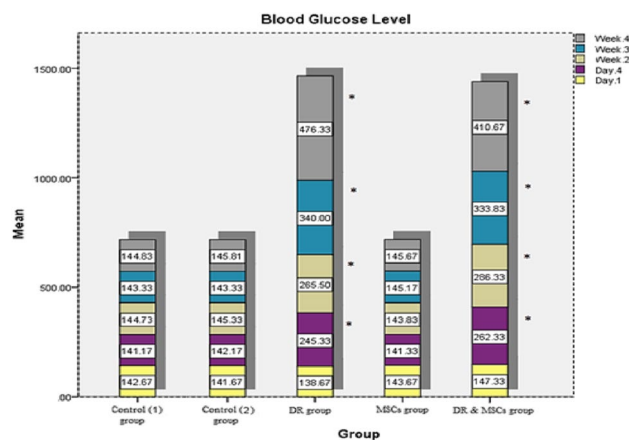


**Fig. 2** Comparison between means of blood glucose level in different experimental groups at days 1 and 4 and in weeks 2, 3, and 4. \* $P=0.001$  versus control groups

appeared in 10 layers; from the choroid to the vitreous, (1) retinal pigment epithelium (RPE) appeared as one layer of cuboidal cells, (2) rods and cones layer (RCL) was a prominent and parallel layer and shows the outer and inner segment of the photoreceptors, (3) outer limiting membrane (OLM) was masked by the cell bodies of the rods and cones, and (4) outer nuclear layer (ONL) appeared in a thick multilayered palisadic arrangement by the nuclei of rods and cones. (5) Outer plexiform layer (OPL) was thin and lightly stained, (6) inner nuclear layer (INL) appeared as multi-layer oval-shaped cells, (7) inner plexiform layer (IPL) was a relatively thick and lightly stained, (8) ganglion cell layer (GCL) contained oval-shaped cells arranged in multilayer, (9) nerve fiber layer (NFL) was thin and lightly stained, and (10) The inner limiting membrane (ILM) was eosinophilic and deeply stained (Fig. 5A and B).

Group III (diabetic retinopathy group) revealed many deep eosinophilic thick-walled small blood vessels (micro-angiopathies) that were detected around the ganglion cells in all animals, eosinophilic vacuolation (exudate) in the OPL in 83% of the animals, and atrophy in the area corresponding to

**Table 1** Mean of body weight in different experimental groups

	Week 1	Week 2	Week 3	Week 4
	Mean ± SD	Mean ± SD	Mean ± SD	Mean ± SD
Control (1) group	211.7 ± 8.8	213.4 ± 6.15	214.67 ± 3.9	216.3 ± 5.7
Control (2) group	211.6 ± 6.8	212.3 ± 6.05	214.7 ± 2.2	216.5 ± 5.2
Diabetic retinopathy group	224 ± 10.13	244.3* ± 9.04	264* ± 8.7	276* ± 10.4
Mesenchymal stem cells group	212.3 ± 10.3	213.8 ± 10.2	214.5 ± 10.4	216.1 ± 9.9
Diabetic retinopathy and mesenchymal stem cells group	225.6 ± 6.44	246.8* ± 18.3	259.2* ± 11.2	273.6* ± 13.9

ANOVA is statistically significant at level of confidence of 95%

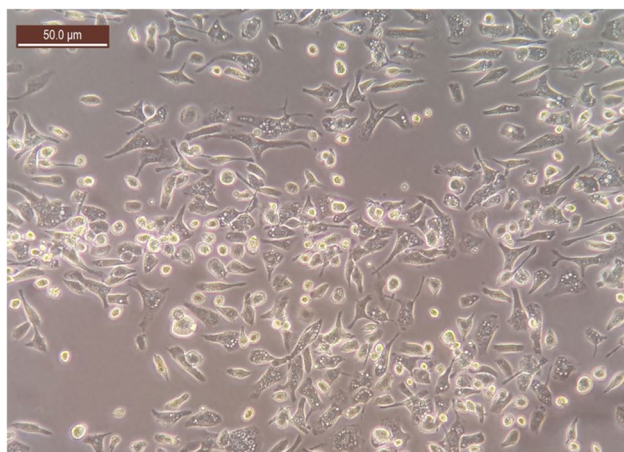
\*Statistically significant difference between these groups and control groups

**Table 2** Mean of blood glucose level in different experimental groups

	Day 1	Day 4	Week 2	Week 3	Week 4
	Mean $\pm$ SD	Mean $\pm$ SD	Mean $\pm$ SD	Mean $\pm$ SD	Mean $\pm$ SD
Control (1) group	142.6 $\pm$ 5.7	141.1 $\pm$ 8.9	144.7 $\pm$ 5.1	143.3 $\pm$ 7.9	144.8 $\pm$ 9.7
Control (2) group	141.6 $\pm$ 5.3	142.1 $\pm$ 7.7	145.3 $\pm$ 4.4	143.3 $\pm$ 7.2	145.8 $\pm$ 3.4
Diabetic retinopathy group	138.6 $\pm$ 6.1	245.3* $\pm$ 30.8	265.5* $\pm$ 38.6	340* $\pm$ 57.1	476.3* $\pm$ 40.9
Mesenchymal stem cells group	143.6 $\pm$ 5.1	141.3 $\pm$ 3.8	143.8 $\pm$ 3.8	145.1 $\pm$ 3.6	145.6 $\pm$ 3
Diabetic retinopathy and mesenchymal stem cells group	147.3 $\pm$ 5	262.3* $\pm$ 34.1	286.3* $\pm$ 42.1	333.8* $\pm$ 46.5	410.6* $\pm$ 26.2

ANOVA is statistically significant at level of confidence of 95%

\*Statistically significant difference between these groups and control groups

**Fig. 3** Phase contrast photomicrography of 60–70% confluent rat BM-MSCs after 7 days of plating showing fibroblastic morphology in the form of spindle-shaped cells (inverted microscope  $\times$  200)

the NFL in 83% of the animals. No intraretinal or extraretinal hemorrhage or retinal detachment was seen in all animals (Fig. 5C1 and Table 5). Degeneration in the inner segment of the photoreceptors in 67% of the animals and patchy degeneration of neurons in the ONL and INL were also seen (Fig. 5C2 and Table 5). In group IV (mesenchymal stem cells group), retinas showed findings similar to control groups (Fig. 5D). In group V (diabetic retinopathy and MSCs group), the cellular organization of the retinal layers appeared

nearly normal. There was also minimal neuronal cell loss in the ONL and INL and moderate eosinophilic vacuolation (exudate) in the OPL in 33% of animals. Less intraretinal microangiopathies were seen around the ganglion cells in comparison to group (III) (Fig. 5E and Table 5).

There was a statistically significant decrease in the GCC and ONL, INL, GCL, and NFL thickness in DR group in comparison to other experimental groups ( $P=0.0001$ ). There was a significant decrease in the ONL, INL, and GCL thickness in DR and MSCs group in comparison to control groups ( $P=0.0001$ ) and no significant difference in the GCC ( $P=0.558$ ) and NFL thickness ( $P=0.996$ ) in DR and MSCs group in comparison to control (1) group (Fig. 6 and Table 3).

### Phosphotungstic Acid (PTAH)

Stained sections from groups I and II (control groups) revealed few deep basophilic neuroglial fibrils extended across the IPL (Fig. 7A and B). Group III (diabetic retinopathy group) showed many thick neuroglial fibrils (gliosis) extended through the IPL and gradually replacing the neuroretina with a layer of neuroglial fibrils running perpendicular to the retinal surface (Fig. 7C). Group IV (mesenchymal stem cells group) showed findings similar to groups I and II (Fig. 7D). In group V (diabetic retinopathy and MSCs group), less thick neuroglial fibrils extended across the IPL compared to group III (Fig. 7E).

**Table 3** Mean of ganglion cell count (GCC), outer nuclear layer thickness (ONL), inner nuclear layer thickness (INL), ganglion cell layer thickness (GCL), and nerve fiber layer thickness (NFL) in different experimental groups

	GCC	ONL	INL	GCL	NFL
Control (1) group	33.21 $\pm$ 5.51	48.67 $\pm$ 4.83	26.997 $\pm$ 3.99	11.06 $\pm$ 2.01	8.20 $\pm$ 1.31
Control (2) group	32.28 $\pm$ 6.67	48.47 $\pm$ 3.65	26.995 $\pm$ 3.82	11.02 $\pm$ 1.91	8.12 $\pm$ 1.82
Diabetic retinopathy group	19.31* $\pm$ 6.64	31.44* $\pm$ 2.87	17.11* $\pm$ 1.88	7.24* $\pm$ 2.14	5.48* $\pm$ 1.66
Mesenchymal stem cells group	31.61 $\pm$ 6.82	48.63 $\pm$ 3.73	27.42 $\pm$ 3.46	10.61 $\pm$ 1.89	7.62 $\pm$ 1.96
Diabetic retinopathy and mesenchymal stem cells group	31.01 $\pm$ 5.77	42.77* $\pm$ 3.33	20.51* $\pm$ 3.23	9.586* $\pm$ 1.67	8.05 $\pm$ 1.52

ANOVA is statistically significant at level of confidence of 95%

\*Statistically significant difference between these groups and control groups

**Table 4** Mean of optical density of the CD34 stained endothelial cells and optical density of the fibronectin immunostained areas in different experimental groups

	CD34 Mean $\pm$ SD	Fibronectin Mean $\pm$ SD
Control (1) group	0.005 $\pm$ 0.002	0.111 $\pm$ 0.06
Control (2) group	0.005 $\pm$ 0.001	0.110 $\pm$ 0.05
Diabetic retinopathy group	0.059* $\pm$ 0.18	0.469* $\pm$ 0.15
Mesenchymal stem cells group	0.005 $\pm$ 0.001	0.114 $\pm$ 0.05
Diabetic retinopathy and mesenchymal stem cells group	0.035* $\pm$ 0.008	0.186* $\pm$ 0.07

ANOVA is statistically significant at level of confidence of 95%

\*Statistically significant difference between these groups and control groups

## Histochemical Findings

### Periodic Acid Schiff (PAS) Stained Sections

Stained sections in groups I and II (control groups) showed dense PAS magenta colored reaction in the ILM and pale magenta colored reaction in the OLM (Fig. 8A and B). Group III (diabetic retinopathy group) revealed disrupted ILM and no obvious changes in the OLM (Fig. 8C). Group IV (mesenchymal stem cells group) revealed findings similar to control

groups (Fig. 8D). Group V (diabetic retinopathy and MSCs group) revealed preserved integrity of ILM and pale reaction in the OLM, similar to groups I, II, and IV (Fig. 8E).

## Immunohistochemical Findings

### Immunostaining of the Retinal Vasculature (CD34)

Stained sections in groups I and II (control groups) revealed negative immunoreaction in the retina in all animals (Fig. 9A and B). Group III (diabetic retinopathy group) showed strong brown positive immunoreaction in all animals in the cell membrane of the endothelial cells of the blood vessels in GCL (Fig. 9C). In group IV (mesenchymal stem cells group), negative immunoreaction was seen in all animals (Fig. 9D). Group V (diabetic retinopathy and MSCs group) showed moderate brown positive immunoreaction in the cell membrane of the endothelial cells compared to group III (Fig. 9E).

There was no significant difference between MSCs group in comparison to control (1) group ( $P = 0.998$ ). There was a significant increase in the CD34 stained endothelial cells in DR group and DR and MSCs group in comparison to control groups ( $P = 0.0001$ ). There was a significant increase in the CD34 stained endothelial cells in DR group in comparison to DR and MSCs group ( $P = 0.0001$ ) (Fig. 10 and Table 4).

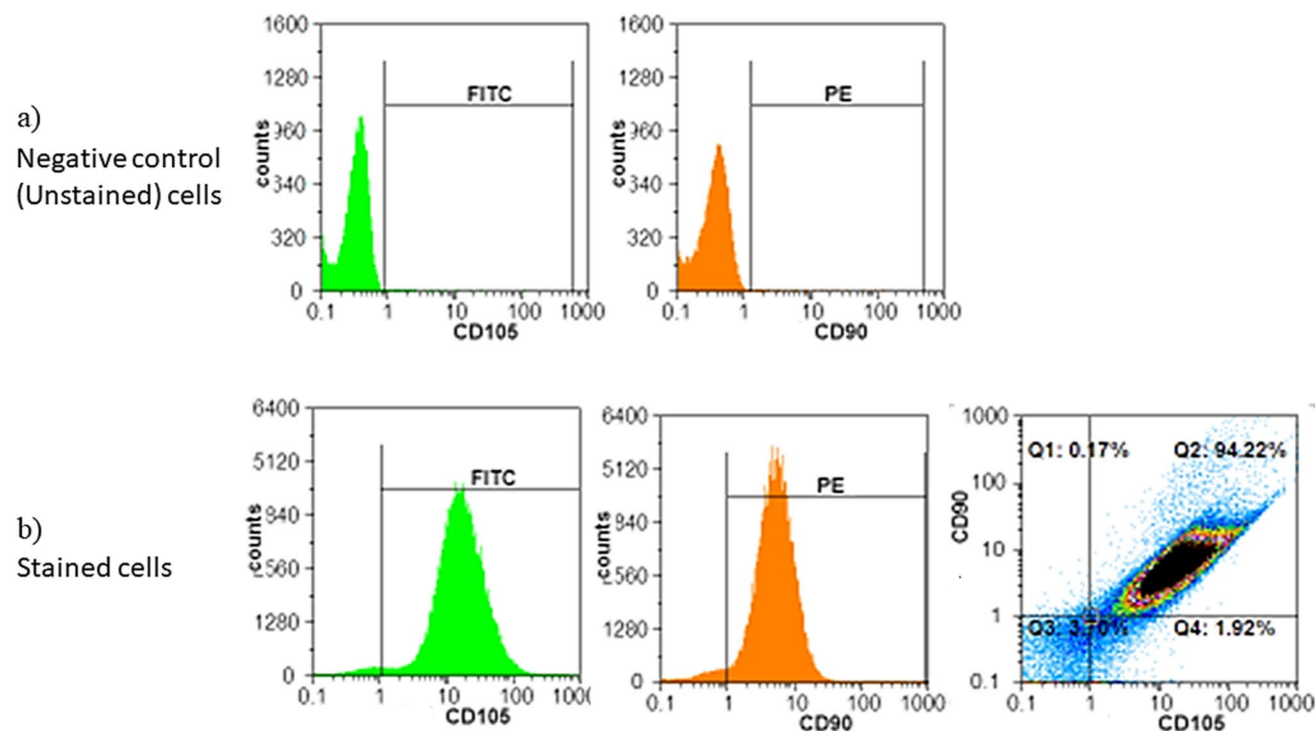


**Fig. 4** A scatter plot represents the BM-MSCs immunophenotyping by flow cytometry, showing **a** negative control cells and **b** 94.22% of cells, which are double positive for CD105 and CD90 surface markers

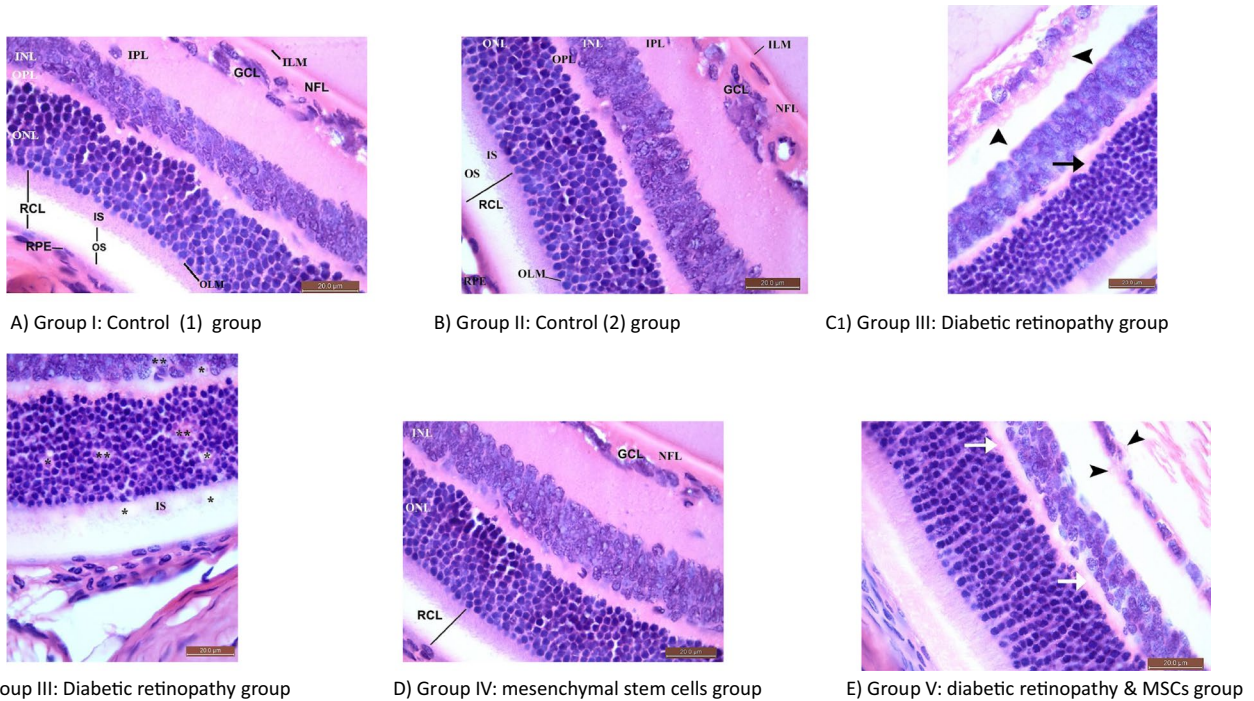


**Fig. 5** Photomicrographs of the retina of control groups, diabetic retinopathy group, mesenchymal stem cells group, and diabetic retinopathy and MSCs group at day 30 (H&E  $\times 1000$ ). **A, B** All retinal layers are shown; retinal pigment epithelium (RPE); rods and cones layer (RCL) contains the outer segment (OS) and inner segment (IS) of the photoreceptors, outer limiting membrane (OLM), outer nuclear layer (ONL), outer plexiform layer (OPL), inner nuclear layer (INL), inner plexiform layer (IPL), ganglion cell layer (GCL), nerve fiber layer (NFL), and inner limiting membrane (ILM). **C1** Small thick-walled blood vessels surrounding the ganglion cells (arrowhead),

eosinophilic vacuolation (exudate) in the OPL (arrow), and atrophy in the area corresponding to the NFL are shown. No intraretinal or extraretinal hemorrhage or retinal detachment is shown. **C2** Disruption of the inner segment (IS) of the photoreceptors and patchy degeneration of neurons in the ONL and INL (stars). **D** Preserved retinal integrity similar to groups I and II. **E** The cellular organization of the retinal layers appeared nearly normal. Minimal neuronal cell loss in the outer nuclear layer (ONL) and inner nuclear layer (INL). Few blood vessels around the ganglion cells (arrowhead) and moderate vacuolation (exudate) in OPL compared to group III (arrow)

**Table 5** Frequency distribution of the histopathological and immunohistochemical findings in different experimental groups

Findings	Groups			
	Controls	Diabetic retinopathy	Mesenchymal stem cell	DR and MSCs
Photoreceptor inner segment degeneration	0%	67%	0%	0%
Vacuolation (exudate) in the outer plexiform layer	0%	83%	0%	33%
Nerve fiber layer		Atrophy	83%	17%
		Hypertrophy	0%	0%
Fibronectin		Diffuse	100%	67%
		Patchy	0%	33%

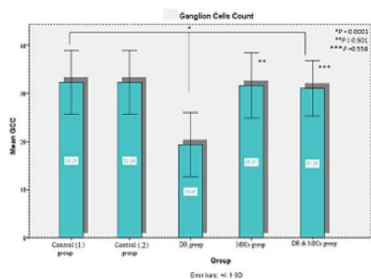
### Immunohistochemical Analysis for Apoptosis (Caspase-3 Active)

Stained sections in groups I and II (control groups) revealed negative immunoreaction in the nuclei of the ganglion cells in all animals (Fig. 11A and B). Group III (diabetic retinopathy group) showed strong brown positive

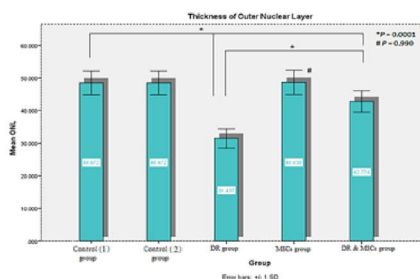
immunoreaction in the nuclei of the ganglion cells in all animals (Fig. 11C). In group IV (mesenchymal stem cells group), negative immunoreaction was seen in all animals as in groups I and II (Fig. 11D). Group V (diabetic retinopathy and MSCs group) showed mild brown positive immunoreaction in the nuclei of the ganglion cells in comparison to the group III (Fig. 11E).



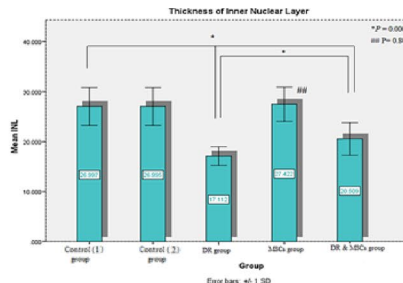
**a)** \* $P = 0.0001$ , \*\* $P = 0.901$  and \*\*\* $P = 0.558$  statistically significant difference between these groups and control (1) group.



**b)** \* $P = 0.0001$  statistically significant difference between these groups and control (1) / DR group. #  $P = 0.990$  statistically significant difference between MSCs group and control (1) group.

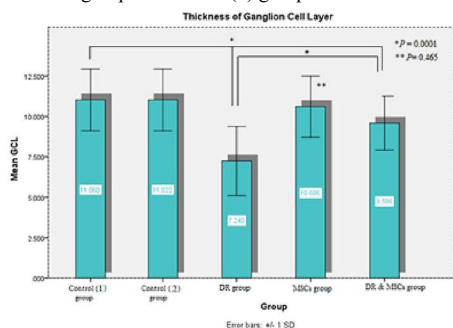


**c)** \* $P = 0.0001$  statistically significant difference between these groups and control (1) / DR group. ##  $P = 0.806$  statistically significant difference between MSCs group and control (1) group.



**d)** \* $P = 0.0001$  statistically significant difference between these groups and control (1) / DR group.

\*\* $P = 0.465$  statistically significant difference between MSCs group and control (1) group.



**e)** \* $P = 0.0001$ , \*\* $P = 0.255$  and \*\*\* $P = 0.996$  statistically significant difference between these groups and control (1) group.

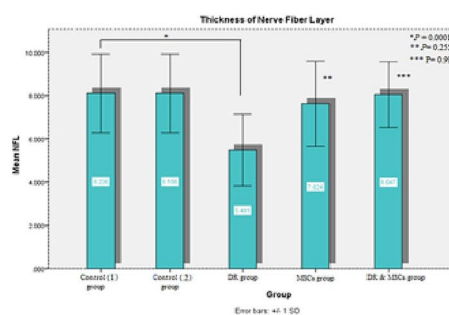


**Fig. 6** Comparison between means of the **a** ganglion cell count (GCC), **b** outer nuclear layer thickness (ONL), **c** inner nuclear layer thickness (INL), **d** ganglion cell layer thickness (GCL), and **e** nerve fiber layer thickness (NFL) in different experimental groups

### Immunohistochemical Analysis for Retinal Fibrosis (Fibronectin)

Stained sections in groups I and II (control groups) revealed mild diffuse positive immunoreaction in all animals in the extracellular space between cells of the ONL (Fig. 12A and B). Group III (diabetic retinopathy group) showed strong patchy brown immunoreaction in all animals between the cells of the ONL and mild brown reaction in the INL in comparison to groups I and II (Fig. 12C and Table 5). In group IV (mesenchymal stem cells group), sections revealed findings similar to groups I and II (Fig. 12D). Group V (diabetic retinopathy and MSCs group) showed moderate brown immunoreaction in the extracellular space between cells of the ONL compared to group III. The reaction was diffuse in 67% of animals and patchy in 33% of animals (Fig. 12E and Table 5).

There was no significant difference between MSCs group in comparison to control (1) group ( $P = 0.997$ ). There was a significant increase in the fibronectin immunostained areas in DR group and DR and MSCs group

in comparison to control groups ( $P = 0.0001$ ). There was a significant increase in the fibronectin immunostained areas in DR group in comparison to DR and MSCs group ( $P = 0.0001$ ) (Fig. 13 and Table 4).

### Polymerase Chain Reaction

The PCR product was amplified from female rats in group V at day 30. All samples were positive for the presence of SRY gene (Fig. 14).

### Discussion

Diabetic retinopathy is the leading obstacle of visual microvascular system injury in diabetic patients. Although microvascular impairment is a central pathological outcome of this condition, in recent years, it has become clearer that diabetes as well has a major impact on the function of retinal neurons and glial cells [29].

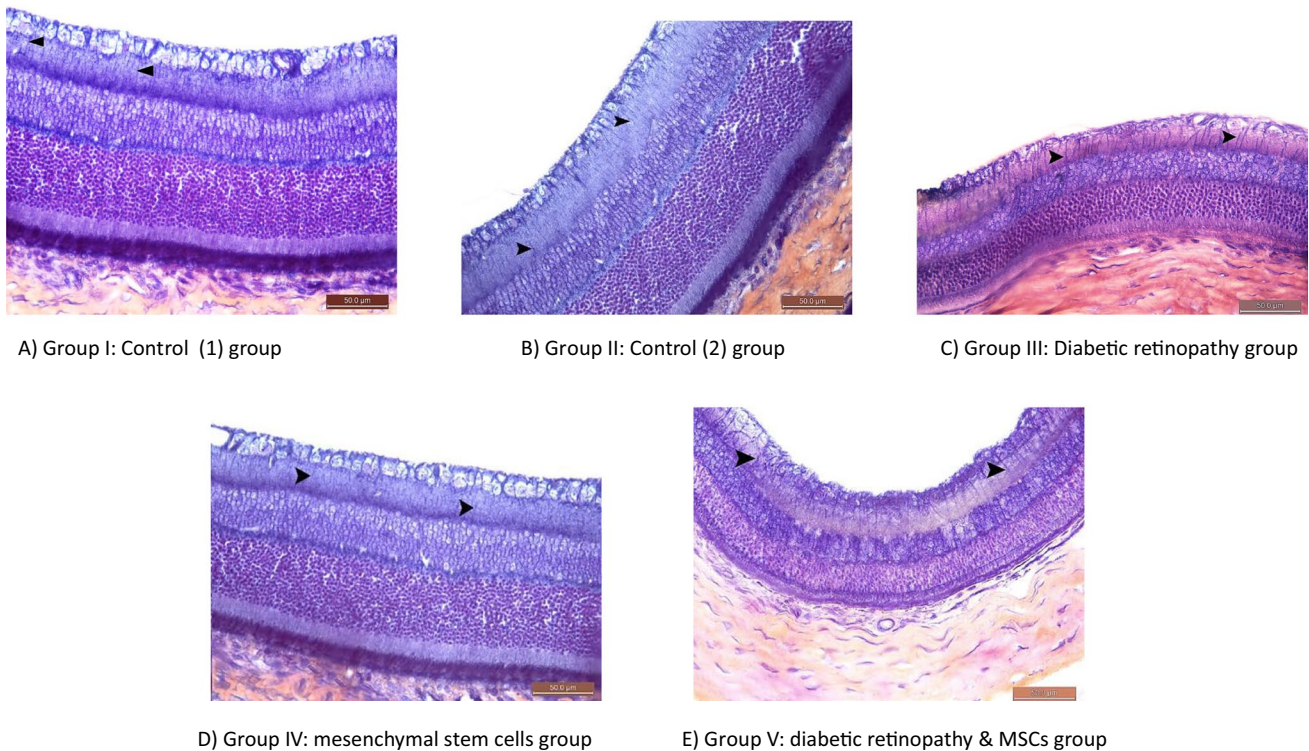


**Fig. 7** Photomicrographs of the retina of control groups, diabetic retinopathy group, mesenchymal stem cells group, and diabetic retinopathy and MSCs group at day 30 (PTAH $\times$ 400). **A, B** Few deep basophilic neuroglial fibrils extend across the IPL (arrowhead). **C** Many thick neuroglial fibrils extending across the IPL (arrowhead) in

comparison to groups I and II and gradually replacing the neuroretina with a layer of neuroglial fibrils running perpendicular to the retinal surface. **D** Few neuroglial fibrils extend across the IPL (arrowhead) similar to groups I and II. **E** Few thick neuroglial fibrils extend across the IPL (arrowhead) compared group III

Though the current treatments ease the advanced irreversible vision loss in severe DR, they are not intended for the early stage of retinopathies [30]. Therefore, there is a need for regenerative disease-modifying therapeutics that can preserve the retinal neurovascular unit in the early stage of the disease.

In an attempt to identify the possible effect of stem cell therapy on the retinal vasculopathy and neuropathy in a short-term experimental diabetes model, we assessed the curative effect of intravitreally injected BM-MSCs on experimentally induced diabetic retinopathy.

On light microscopic examination, our study revealed severe histopathological changes in the DR group. Although most of the changes were present in all animals, there were some variations in the severity of the lesions. In the H&E stained sections, our results were consistent with many studies such as those of Szabó et al. [25], Enzsoly et al. [31], and Park et al. [32] whose results showed signs of photoreceptor apoptosis in different diabetic rat strains after diabetes induction. Enzsoly et al. [31] explained the effect on the photoreceptors by the failure of secretion of different growth factors from the RPE.

Cell loss in different retinal layers, found in our study, may be due to several mechanisms including oxidative stress, microglia activation, perfused capillaries, and the release of vasodilator; all can induce disturbance in the blood supply of neurons [24]. Additionally, microRNA-133b overexpression was found to inhibit retinal cell proliferation and promote their apoptosis in DR animal models [33]. Also, inappropriate activation of the inflammasome and apoptosis-associated speck-like protein containing a C-terminal caspase activation lead to continuous cell loss in different retinal layers [34]. In accordance with our results, Zhang et al. [28] and Nakahara et al. [35] detected marked thinning of the different retinal layers after diabetes induction which was confirmed by Qu et al. [11] who found detectable atrophy in the ONL. In addition, it was reported that neuronal cell apoptosis and axonal degeneration may be due to Muller cell dysfunction which led to inappropriate osmotic stability between the intra- and the extracellular matrices [36].

Chen et al. [37] clarified that exudate accumulation is generated by hyperglycemia-induced junctional adhesion molecules downregulation in retinal endothelial cells leading to loss of the structural integrity of the tight junction

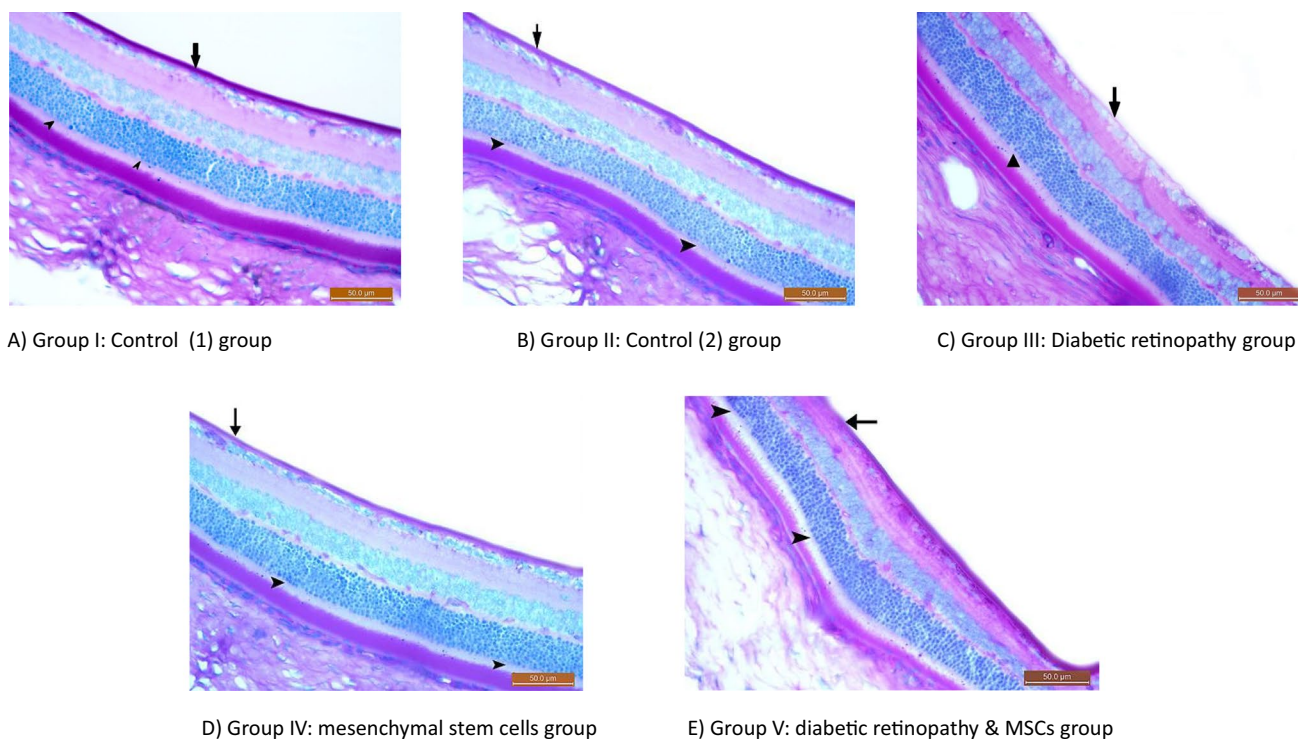


**Fig. 8** Photomicrographs of the retina of control groups, diabetic retinopathy group, mesenchymal stem cells group, and diabetic retinopathy and MSCs group at day 30 (PAS×400). **A, B** Dense PAS reaction in the ILM (arrow) and pale PAS reaction in the OLM

(arrowhead). **C** Disrupted ILM (arrow) and no obvious changes in the OLM (arrowhead). **D** Similar to the groups I and II. **E** Preserved integrity of ILM (arrow) and pale PAS reaction in the OLM (arrowhead)

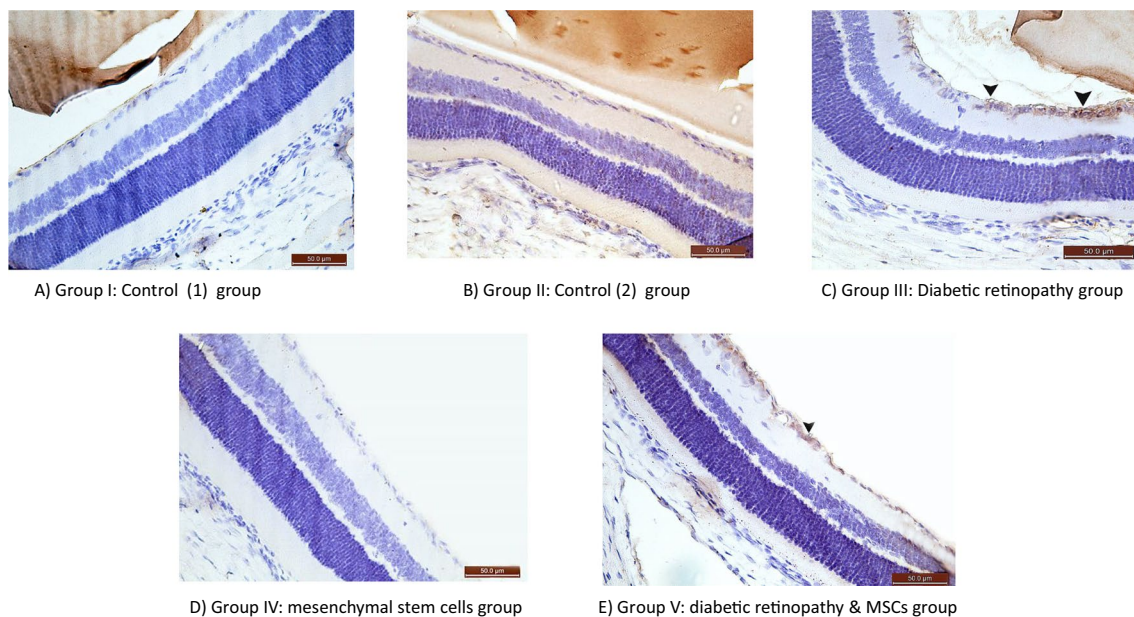


**Fig. 9** Photomicrographs of the retina of control groups, diabetic retinopathy group, mesenchymal stem cells group, and diabetic retinopathy and MSCs group at day 30 (CD34 immunohistochemical stain×400). **A, B** Negative immunoreaction is shown. **C** Strong

brown positive immunoreaction in the cell membrane of the endothelial cells of the blood vessels in the GCL (arrowhead). **D** Similar to the groups I and II. **E** Moderate brown positive immunoreaction in the cell membrane of the endothelial cell in the GCL (arrowhead)

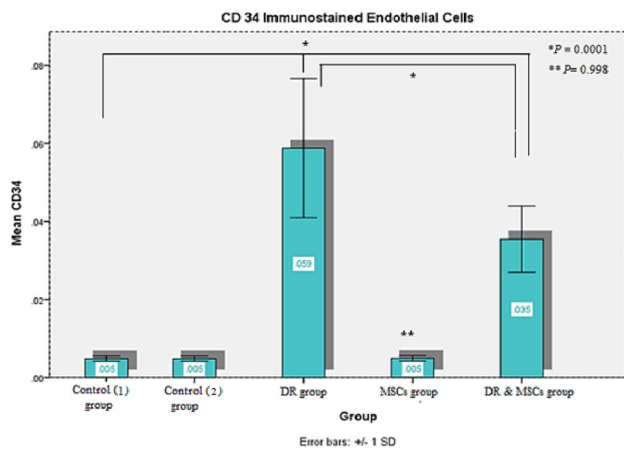


**Fig. 10** Comparison between means of the optical density of CD34 immunohistochemical stained cells among different experimental groups. \* $P=0.0001$  statistically significant difference between these groups and control (1)/DR group. \*\* $P=0.998$  statistically significant difference between MSCs group and control (1) group

between cells. Another important mechanism can be through destruction in RPEs' junctional complex [38]. These metabolic alternations triggering chronic inflammation causing blood-retinal barrier (BRB) damage increase capillary non-perfusion and later edema [39]. The inflamed retina has an increased level of adhesion molecules, cytokines, and chemokines. In turn, leukostasis occurs which contributes to further microvascular damage and vascular leakage [40].

In the PTAH stained sections, our finding was documented in many studies such as that conducted by McDowell et al. [29] who found gliosis extensively extended in the IPL in STZ-diabetic rats. The most accepted explanation is that hyperglycemia causes regular  $K^+$  and fluid uptake by Muller cells without releasing them into the vitreous humor or the microvasculature respectively. This leads to failure in the osmotic fluid removal and subsequently Muller cell swelling and gliosis [36, 41, 42].

In the PAS stained sections, our result was consistent with Ashraf, Souka, and Adelman [43] and Daruich et al. [38] results. They reported that hyperglycemia aids in the disruption of limiting membranes through distracting the tight junction protein complexes in the membranes.

Our CD34 immunohistochemical results were similar to those of Liu et al. [24], who reported increase in the number of CD34-positive endothelial cells in DR group compared to control group. It was reported that hyperglycemia influences angiogenesis through the modulation of various factors, such as VEGF, fibroblast growth factor, and angiotensin [24, 44]. Excessive production of VEGF increases microRNA-155 expression, which, in turn, prevents endothelial cell apoptosis and creates pathological neovascularization [41]. In addition, the hypoxic environment in DR leads to a decreased amount of microRNA-150-5p and an increased amount of both microRNA-21-3p and microRNA-30b-5p, which both promote neovascularization and encourage angiogenesis [45].

In accordance with our results in caspase-3 active immunohistochemical stain, Enzoly et al. [31] detected sporadic

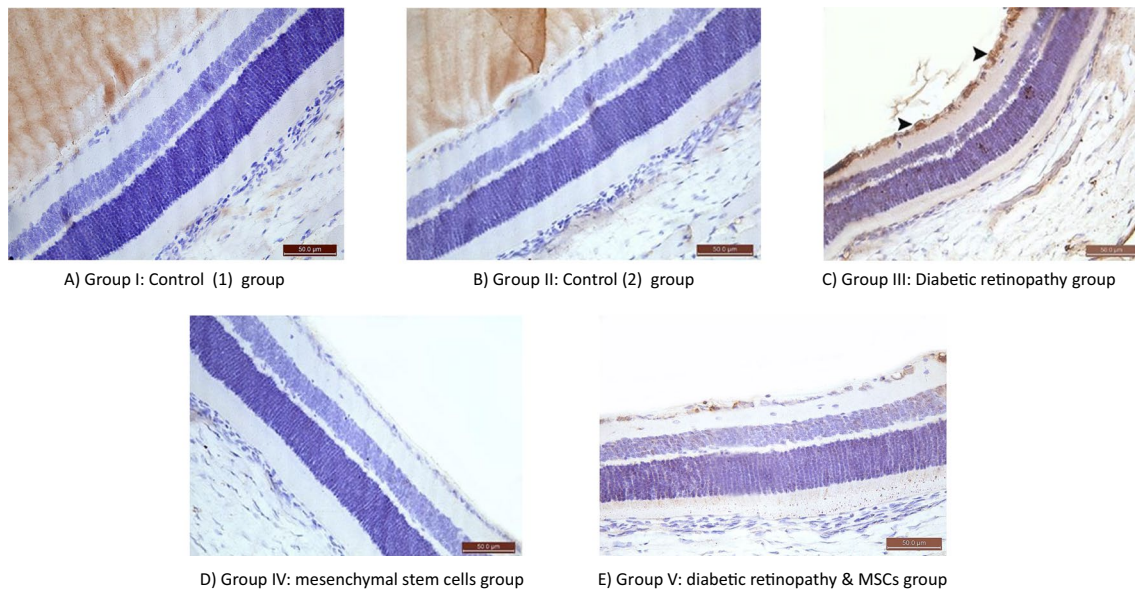


**Fig. 11** Photomicrographs of the retina of control groups, diabetic retinopathy group, mesenchymal stem cells group, and diabetic retinopathy and MSCs group at day 30 (caspase-3 active immunohistochemical stain  $\times 400$ ). **A, B** Negative immunoreaction in the GCL. **C**

Strong brown positive immunoreaction in the nuclei of ganglion cells (arrowhead). **D** Negative immunoreaction in the nuclei of the ganglion cells similar to groups I and II. **E** Mild brown positive immunoreactions in the nuclei of the ganglion cells

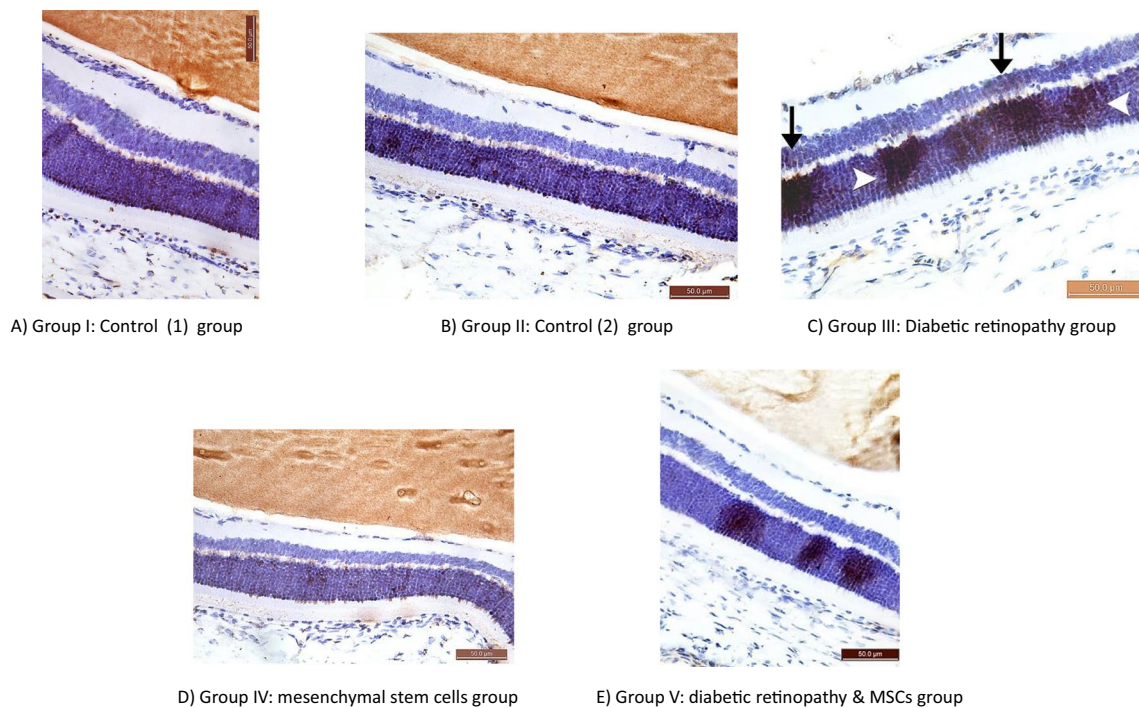


**Fig. 12** Photomicrographs of the retina of control groups, diabetic retinopathy group, mesenchymal stem cells group, and diabetic retinopathy and MSCs group at day 30 (fibronectin immunohistochemical stain  $\times 400$ ). **A, B** Mild diffuse brown immunoreaction between cells of the ONL. **C** Strong patchy brown immunoreaction in the extracel-

lular space between cells of the ONL (arrowhead) and mild reaction in the INL (arrow). **D** Similar to groups I and II. **E** Moderate patchy brown positive immunoreaction in the extracellular space between cells of the ONL

TUNEL-positive reaction in the GCL, INL, and ONL after STZ induction of diabetes. This finding was explained by the accumulation advanced glycation end products (AGEs) that have a direct association with neuronal cell apoptosis [46].

The increase in fibronectin immunohistochemical reaction in our study was also detected by Zhou et al. [47], in STZ-diabetic mice after 16 weeks of the onset of diabetes. This was explained by the influence of endothelial-mesenchymal transition on the development of fibroblasts and myofibroblasts leading to fibrosis [44, 48].

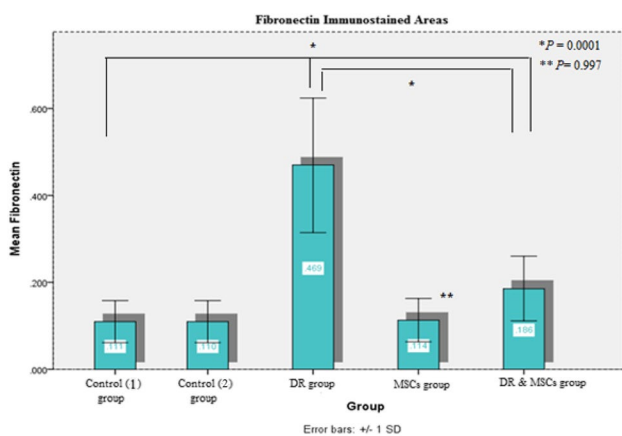
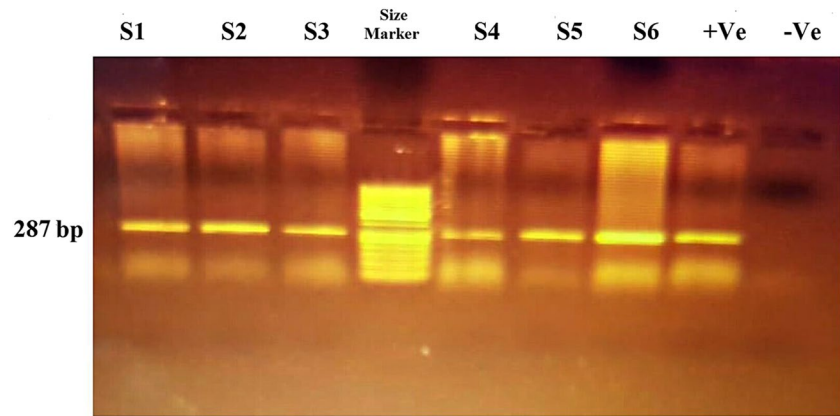


**Fig. 13** Comparison between means of the optical density of fibronectin immunohistochemical stained areas among different experimental groups.  $*P=0.0001$  statistically significant difference between these groups and control (1)/DR group.  $**P=0.997$  statistically significant difference between MSCs group and control (1) group

In DR and MSCs group, our findings for H&E stained sections were in agreement with Na et al. [49] who found a great improvement in the treated retinas following the local injection of BM-MSCs in a retinal ischemia animal model. Other studies such as Rajashekhar [50], Elshaer et al. [30], and Safwat et al. [51] using adipose MSCs proved that MSCs restored the cellular component of the retina and were able to protect retinal neurons in STZ-induced DR.

Good efficacy of BM-MSCs might be related to several mechanisms. Kramerov and Ljubimov [52] claimed that MSCs can absorb the reactive oxygen species created from the oxidative stress. Also, Zhang and Wang [53] demonstrated that BM-MSCs released neurotrophic growth factors that inhibit apoptosis, stimulate angiogenesis, and regenerate the neurovascular retinal tissue. As well, Elshaer et al. [30] mentioned that BM-MSCs control the immuno-regulators at the site of injury while instantaneously initiating tissue remodeling.

**Fig. 14** A photomicrograph of gel electrophoresis showing PCR-amplified SRY gene from the DNA samples of group V at day 30. Lane 4, size marker; lanes 1–3, 5–7, positive samples from the eyes; lane 8, positive control for the gene; and lane 9, negative control for the gene



In agreement with our results, Qu et al. [11] detected a significant increase in the thickness of ONL at week 3 after BM-MSCs transplantation. The decrease in retinal cell loss and increase in retinal layer thickness (ONL, INL, and GCL), in our study, compared to the DR group, can be attributed to the trophic factors, immunomodulators, and exosomes secreted by the BM-MSCs during the first few days following cell injection [22].

Similar to our PTAH result, Çerman et al. [14] noted that BM-MSCs integrated into the inner retina layer stimulated gliosis in rat models of DR. This may be due to the ability of the intravitreally transplanted BM-MSCs to differentiate to Muller glia, or to release microvesicles that induce differentiation of native Muller cells [14].

Our findings of CD34 immunohistochemical stained sections were also reported by Ezquer et al. [54]. They explained this by the significant increase in thrombospondin-1 and anti-angiogenic factor in the treated group compared to both diabetic and control groups.

Safwat et al. [51] suggested that hyperglycemia decreased the level of microRNA-222 expression which inhibits neovascularization and modulates vascular smooth muscle cell proliferation. Also, Xu et al. [16] findings revealed that the expression of microRNA-18b was significantly elevated in the retinas of diabetic rats after MSCs-EV treatment. MicroRNA-18b was found to target mitogen-activated protein kinase kinase kinase-1 (MAP3K1), thus reducing inflammation and cellular apoptosis. da Silva-Junior et al. [55] demonstrated that MSCs had a sustained neuroprotective effect on the retinal ganglion cells after optic nerve crush in a rat model. Likewise, Mathew et al. [56] detected a preserved amount of the ganglion cells in rats receiving intravitreal injection of MSCs-EVs compared to retinal ischemia model. An important mechanism by which MSCs can reduce ganglion cell apoptosis in DR rats was illustrated by Mead and Tomarev [12] who suggested that the EV effects on neuronal cell apoptosis are either due to the retinal cell to cell signaling or due to the release of anti-apoptotic factors from the cells that have endocytosed the EVs.

Using fibronectin immunohistochemical stain, in consistency with our results, Wang et al. [15] detected no significant difference between the treated group and the control group after intravitreal injection of BM-MSCs in STZ-diabetic rats, indicating reduction in the vascular leakage and decrease in young fibroblast proliferation which synthesize the components of the extracellular matrix.

During early DR, AGEs and VEGF increase expression of CTGF that in turn increases fibronectin ECM deposition. MSCs have been shown to reverse the alterations of ECM proteins and express greater amounts of MMP3 that were capable of degrading CTGF and altering myofibroblast differentiation towards endothelial lineage cells, and this process contributes to retinal repair [13].

Our results were supported by thermal cycler PCR results which ascertain homing of the intravitreally injected BM-MSCs. Male-specific marker, SRY gene, located on the Y chromosome was used to identify male donor-derived cells in female recipients. The results revealed that all samples of female recipient rats in DR and MSCs group contained male-specific SRY gene. However, the location and the amount of the injected BM-MSCs within the retina could not be confirmed.

Despite the curative effect of BM-MSCs, the present study has pointed out so far that BM-MSCs, in general, are safe. No serious adverse reaction was reported in the MSCs group.

## Limitations

Our study has some limitations. First, no gross examination of the developed diabetic retinopathy was performed. This could be justified by the fact that we focused on the histopathological analysis and no ophthalmologists were included in our team for conducting the gross examination. Second is the short-term duration of our study. Further studies are recommended to include gross retinal examination of the developing diabetic retinopathy. Additionally, further preclinical

studies are recommended to establish long-term safety, tolerability, and effectiveness of cell therapy versus the risk of adverse effects.

## Conclusion

Overall, intravitreally injected BM-MSCs showed a partial protective effect on the retinal neurovascular unit in diabetic rats through decreasing retinal damage, as well as maintaining neural cells survival. This may be due to the failure of some BM-MSCs to penetrate the ILM, which remained either in the vitreous or on the retinal surface.

**Abbreviations** AGEs: advanced glycation end products; BM-MSCs: bone marrow mesenchymal stem cells; BRB: blood-retinal barrier; CTGF: connective tissue growth factor; DR: diabetic retinopathy; ECM: extracellular matrix; EDTA: ethylene diamine tetra-acetate; EVs: extracellular vesicles; FC: fragment crystallizable; GCL: ganglion cell layer; GFAP: glial fibrillary acidic protein; H&E: hematoxylin and eosin; ILM: inner limiting membrane; INL: inner nuclear layer; IPL: inner plexiform layer; MAP3K1: mitogen-activated protein kinase kinase kinase-1; MMPs: matrix metalloproteases; NFL: nerve fiber layer; OLM: outer limiting membrane; ONL: outer nuclear layer; OPL: outer plexiform layer; PAS: periodic acid Schiff; PATH: phosphotungstic acid-hematoxylin; PBS: phosphate buffer saline; RCL: rods and cones layer; RPE: retinal pigment epithelium; STZ: streptozotocin; VEGF: vascular endothelial growth factor

**Acknowledgements** The authors thank Associate Prof. Eman Ali Toraih and Dr. Noha M. Abd El-Fadeal for their help through this work.

**Author Contribution** Nahla Imbarak participated in the study design; carried out stem cell isolation, culture and characterization using flow cytometry, PCR analysis, collection and assembly of data, data analysis and interpretation; and drafted the manuscript. Horeya Erfan Korayem participated in the study design and collection and assembly of data. Nema Soliman participated in the study design and data interpretation. Somaya Hosny participated in its design and coordination, and helped in drafting the manuscript. All authors participated in the manuscript writing and approved the final manuscript.

**Data Availability** Data will be available only on reasonable request.

## Declarations

**Ethical Approval** After approval of the Institutional Research Ethics Committee Guidelines (Faculty of Medicine, Suez Canal University) for the care and use of animals, 30 female Wistar albino rats aged 6–7 months and weighing between 200 and 250 g and 10 male albino rats, 4–6 weeks old, weighing around 150 g, were brought from the National Research Center for Experimental Animals, Cairo. One week before the beginning of the experiment, the animals were acclimatized to their place and placed in their cages (one animal/cage). To ensure compliance with ethical considerations, rats were subjected to general anesthesia with intramuscular injection of 75 mg/kg ketamine before intravitreal injection.

**No Informed Consent or Reporting Checklist** The study was carried out on experimental animals.

**Conflict of Interest** The authors declare no competing interests.

## References

- Rübsam A, Parikh S, Fort PE. Role of inflammation in diabetic retinopathy. *Int J Mol Sci* [Internet]. 2018;19:1–31. Available from: <https://www.ncbi.nlm.nih.gov/pmc/articles/PMC5979417/>
- AlSawahli H, Mpyet CD, Ezzelarab G, Hassanin I, Shalaby M, Safa O, et al. Population-based cross-sectional prevalence survey of diabetes and diabetic retinopathy in Sohag-Egypt, 2019. *BMJ Open*. 2021;11:e047757.
- Stitt PAW, Curtis TM, Chen M, Medina RJ, McKay GJ, Jenkins A, et al. The progress in understanding and treatment of diabetic retinopathy. *Prog Retin Eye Res* [Internet]. Elsevier Ltd; 2015;51:1–108. Available from: <https://doi.org/10.1016/j.preteyeres.2015.08.001>
- Ovalle W, Nahirney P. *Netter's essential histology*. 2nd ed. Elsevier Ltd; 2013
- Lieth E, Gardner TW, Barber AJ, Antonetti DA, Penn T, Retina S. Retinal neurodegeneration : early pathology in diabetes. *Clin Exp Ophthalmology* [Internet]. 2000;28:3–8. Available from: <https://onlinelibrary.wiley.com/doi/abs/10.1046/j.1442-9071.2000.00222.x?sid=nlm%3Apubmed>
- Lai AKW, Lo ACY. Animal models of diabetic retinopathy: summary and comparison. *J Diabetes Res* [Internet]. 2013;2013:29. Available from: <https://www.ncbi.nlm.nih.gov/pmc/articles/PMC3826427/>
- Lechner J, O'Leary OE, Stitt AW. The pathology associated with diabetic retinopathy. *Vision Res* [Internet]. Elsevier Ltd; 2017;139:7–14. Available from: <https://doi.org/10.1016/j.visres.2017.04.003>
- Reid E, Guduric-Fuchs J, O'Neill CL, Allen L-D, Chambers SEJ, Stitt AW, et al. Preclinical evaluation and optimization of a cell therapy using human cord blood-derived endothelial colony-forming cells for ischemic retinopathies. *Stem Cells Transl Med* [Internet]. 2018;7:59–67. Available from: <http://doi.wiley.com/10.1002/sctm.17-0187>
- Hartman GD, Lambert-Cheatham NA, Kelley MR, Corson TW. Molecular sciences inhibition of APE1/Ref-1 for neovascular eye diseases: from biology to therapy. 2021; Available from: <https://doi.org/10.3390/ijms221910279>
- Jones MK, Lu B, Girman S, Wang S. Cell-based therapeutic strategies for replacement and preservation in retinal degenerative diseases. *Prog Retin Eye Res* [Internet]. Elsevier Ltd; 2017;58:1–27. Available from: <https://doi.org/10.1016/j.preteyeres.2017.01.004>
- Qu L, Gao L, Xu H, Duan P, Zeng Y, Liu Y, et al. Combined transplantation of human mesenchymal stem cells and human retinal progenitor cells into the subretinal space of RCS rats. *Sci Rep* [Internet]. Springer US; 2017;7:199. Available from: <http://www.nature.com/articles/s41598-017-00241-5>
- Mead B, Tomarev S. Bone marrow-derived mesenchymal stem cells-derived exosomes promote survival of retinal ganglion cells through miRNA-dependent mechanisms. *Stem Cells* [Internet]. 2017;6:1273–85.
- Fiori A, Terlizzi V, Kremer H, Gebauer J, Hammes H, Harmsen MC, et al. Mesenchymal stromal / stem cells as potential therapy in diabetic retinopathy. *Immunobiology* [Internet]. Elsevier; 2018;223:729–43. Available from: <https://doi.org/10.1016/j.imbio.2018.01.001>
- Çerman E, Akkoç T, Eraslan M, Özlem Ş, Özkara S. Retinal electrophysiological effects of intravitreal bone marrow derived mesenchymal stem cells in streptozotocin induced diabetic rats. *PLoS One*. 2016;11(6):e0156495.
- Wang J, An Y, Zhang J, Wan X, Jonas JB, Xu L. Human bone marrow mesenchymal stem cells for retinal vascular injury. *Acta Ophthalmologica* [Internet]. 2017;95:453–61. Available from: <https://onlinelibrary.wiley.com/doi/full/10.1111/aos.13154>

16. Xu Z, Tian N, Li S, Li K, Guo H, Zhang H, et al. Extracellular vesicles secreted from mesenchymal stem cells exert anti-apoptotic and anti-inflammatory effects via transmitting microRNA-18b in rats with diabetic retinopathy. *Int Immunopharmacol*. 2021;101:108234 (Netherlands).
17. Hu B, Zhang Y, Zeng Q, Han Q, Zhang L, Liu M, et al. Intravitreal injection of ranibizumab and CTGF shRNA improves retinal gene expression and microvessel ultrastructure in a rodent model of diabetes. *Int J Mol Sci* [Internet]. 2014;15:1606–24. Available from: <https://www.ncbi.nlm.nih.gov/pmc/articles/PMC3907889/>
18. Li L, Li Y lin, Zhou Y feng, Ge Z yan, Wang L li, Li Z qiang, et al. Jiangtang Xiaozhi Recipe ( ) prevents diabetic retinopathy in streptozotocin-induced diabetic rats. *Chin J Integr Med* [Internet]. 2017;23:425–32. Available from: <https://link.springer.com/article/10.1007%2Fs11655-016-2595-x>
19. Dickinson H, Milton P, Jenkin G. The isolation and characterization of putative mesenchymal stem cells from the spiny mouse. *Cytotechnology* [Internet]. 2012;64:591–9. Available from: <https://www.ncbi.nlm.nih.gov/pmc/articles/PMC3432532/>
20. Wakitani S, T S, Caplan A. Myogenic cells derived from rat bone marrow mesenchymal stem cells exposed to 5-azacytidine. *Muscle Nerve* [Internet]. 1995;18:1417–26. Available from: <https://onlinelibrary.wiley.com/doi/abs/10.1002/mus.880181212>
21. Basiouny HS, Salama NM, Mohamed Z, Maadawi E, Farag EA. Effect of bone marrow derived mesenchymal stem cells on healing of induced full-thickness skin wounds in albino rat. *Int J Stem Cells* [Internet]. 2013;6:12–25. Available from: <https://www.ncbi.nlm.nih.gov/pubmed/24298370>
22. Tzameret A, Sher I, Belkin M, Treves AJ, Meir A, Nagler A, et al. Epiretinal transplantation of human bone marrow mesenchymal stem cells rescues retinal and vision function in a rat model of retinal degeneration. *Stem Cell Res*. 2015;15(2):387–94. <https://doi.org/10.1016/j.scr.2015.08.007>.
23. Gholipour MA, Kanavi MR, Ahmadi H, Aldavood S, Nourinia R, Hosseini S, et al. Original article: intravitreal topotecan inhibits laser - induced choroidal neovascularization in a rat model. *J Ophthalmic Vis Res*. 2015;10(3):295–302.
24. Liu H, Zhou S, Denyer G, Meng Z, Chen R, Lv L, et al. Reduced  $\beta$ 2glycoprotein I inhibits hypoxia-induced retinal angiogenesis in neonatal mice through the vascular endothelial growth factor pathway. *Mol Med Rep* [Internet]. 2015;11:1025–30. Available from: <https://www.spandidos-publications.com/mmr/11/2/1025>
25. Szabó K, Énzöly A, Dékány B, Szabó A, Hajdú RI, Mátyás C, et al. Histological evaluation of diabetic neurodegeneration in the retina of Zucker diabetic fatty ( ZDF ) rats. *Sci Rep* [Internet]. 2017;7:1–17. Available from: <https://www.ncbi.nlm.nih.gov/pmc/articles/PMC5566374/>
26. Issa N, El-sherif N. Histological and immunohistochemical studies on the cornea and retina of sofosbuvir treated rats. *Austin J Anat* [Internet]. 2017;4:1068. Available from: <http://austinpublishinggroup.com/anatomy/fulltext/Anatomy-v4-id1068.php>
27. Imbarak N, Abdel-Aziz HI, Farghaly LM, Hosny S. Effect of mesenchymal stem cells versus aloe vera on healing of deep second-degree burn. *Stem Cell Investig* [Internet]. 2021;8. Available from: <https://pubmed.ncbi.nlm.nih.gov/34268441/>
28. Zhang J, Wu Y, Jin Y, Ji F, Sinclair SH, Luo Y, et al. Intravitreal injection of erythropoietin protects both retinal vascular and neuronal cells in early diabetes. *Investig Ophthalmol Vis Sci* [Internet]. 2008;49:732–42. Available from: <https://iovs.arvojournals.org/article.aspx?articleid=2164222>
29. McDowell RE, Barabas P, Augustine J, Chevallier O, Mccarron P, Chen M, et al. Müller glial dysfunction during diabetic retinopathy in rats is reduced by the acrolein-scavenging drug , 2-hydrazino-4 , 6-dimethylpyrimidine. *Diabetologia* [Internet]. 2018;61:2654–67. Available from: <https://doi.org/10.1007/s00125-018-4707-y%0A>
30. Elshaer SL, Evans W, Pentecost M, Lenin R, Periasamy R, Jha KA, et al. Adipose stem cells and their paracrine factors are therapeutic for early retinal complications of diabetes in the Ins2 Akita mouse. *Stem Cell Res Ther* [Internet]. *Stem Cell Res Ther*; 2018;9:322. Available from: <https://www.ncbi.nlm.nih.gov/pmc/articles/PMC6249931/>
31. Enzsoly A, Szabo A, Kantor O, David C, Szalay P, Szabo K, et al. Pathologic alterations of the outer retina in streptozotocin-induced diabetes. *Investig Ophthalmol Vis Sci* [Internet]. 2014;55:3686–99. Available from: <https://iovs.arvojournals.org/article.aspx?articleid=2128639>
32. Park S-H, Park J-W, Park S-J, Kim K-Y, Chung J-W, Chun M-H, et al. Apoptotic death of photoreceptors in the streptozotocin-induced diabetic rat retina. *Diabetologia* [Internet]. Germany; 2003;46:1260–8. Available from: <https://link.springer.com/article/10.1007%2Fs00125-003-1177-6>
33. Satari M, Aghadavod E, Mirhosseini N, Asemi Z. The effects of microRNAs in activating neovascularization pathways in diabetic retinopathy. *J Cell Biochem* [Internet]. 2018;120:9514–21. Available from: <https://onlinelibrary.wiley.com/doi/abs/10.1002/jcb.28227>
34. Wang M, Wang Y, Xie T, Zhan P, Zou J, Nie X, et al. Prostaglandin E2/EP2 receptor signalling pathway promotes diabetic retinopathy in a rat model of diabetes. *Diabetologia* [Internet]. *Diabetologia*; 2019;62:335–48. Available from: <https://link.springer.com/article/10.1007%2Fs00125-018-4755-3>
35. Nakahara T, Hoshino M, Hoshino S, Mori A, Sakamoto K. Structural and functional changes in retinal vasculature induced by retinal ischemia-reperfusion in rats. *Exp Eye Res* [Internet]. Elsevier Ltd; 2015;135:134–45. Available from: <https://doi.org/10.1016/j.exer.2015.02.020>
36. Vujosevic S, Midena E. Retinal layers changes in human pre-clinical and early clinical diabetic retinopathy support early retinal neuronal and Müller cells alterations. *J Diabetes Res* [Internet]. 2013;2013:1–8. Available from: <https://www.ncbi.nlm.nih.gov/pmc/articles/PMC3694491/>
37. Chen Y, Meng J, Li H, Wei H, Bi F, Liu S, et al. Resveratrol exhibits an effect on attenuating retina inflammatory condition and damage of diabetic retinopathy via PON1. *Exp Eye Res* [Internet]. Elsevier; 2019;181:356–66. Available from: <https://doi.org/10.1016/j.exer.2018.11.023>
38. Daruich A, Matet A, Moulin A, Kowalczyk L, Nicolas M, Sellam A, et al. Mechanisms of macular edema: beyond the surface. *Prog Retin Eye Res* [Internet]. England; 2018;63:20–68. Available from: <https://www.sciencedirect.com/science/article/pii/S1350946217300757?via%3Dihub>
39. Wykoff C. Impact of intravitreal pharmacotherapies including antivascular endothelial growth factor and corticosteroid agents on diabetic retinopathy. *Curr Opin Ophthalmol* [Internet]. 2017;28:213–218. Available from: <https://insights.ovid.com/pubmed?pmid=28376510>
40. Yeh P-T, Huang Y-H, Chang S-W, Wang L-C, Yang C-M, Yang W-S, et al. Cilostazol attenuates retinal oxidative stress and inflammation in a streptozotocin-induced diabetic animal model. *Curr Eye Res* [Internet]. England; 2019;44:294–302. Available from: <https://www.tandfonline.com/doi/abs/10.1080/02713683.2018.1542734?journalCode=icey20>
41. Yang J, Chen C, Mclaughlin T, Wang Y, Le Y, Wang JJ. Loss of X-box binding protein 1 in Müller cells augments retinal inflammation in a mouse model of diabetes. *Diabetologia* [Internet]. *Diabetologia*; 2019;62:531–43. Available from: <https://link.springer.com/article/10.1007%2Fs00125-018-4776-y>
42. Coughlin BA, Feenstra DJ, Mohr S. Müller cells and diabetic retinopathy. *Vision Res* [Internet]. 2017;139:93–100. Available from: <https://www.ncbi.nlm.nih.gov/pmc/articles/PMC5794018/>
43. Ashraf M, Souka A, Adelman R. Predicting outcomes to anti-vascular endothelial growth factor (VEGF) therapy in diabetic



- macular oedema: a review of the literature. *Br J Ophthalmol* [Internet]. England; 2016;100:1596–604. Available from: <https://www.ncbi.nlm.nih.gov/pubmed/?term=10.1136%2Fbjophthamol-2016-308388>
44. Thomas AA, Biswas S, Feng B, Chen S, Gonder J, Chakrabarti S. lncRNA H19 prevents endothelial – mesenchymal transition in diabetic retinopathy. *Diabetologia* [Internet]. Springer- Verlag GmbH Germany; 2019;62:517–30. Available from: <https://doi.org/10.1007/s00125-018-4797-6/0AARTICLE%0AlncRNA>
  45. Mazzeo A, Lopatina T, Gai C, Trento M, Porta M, Beltramo E. Functional analysis of miR-21–3p, miR-30b-5p and miR-150–5p shuttled by extracellular vesicles from diabetic subjects reveals their association with diabetic retinopathy. *Exp Eye Res* [Internet]. England; 2019;184:56–63. Available from: <https://www.sciencedirect.com/science/article/pii/S0014483518308376?via%3DIihub>
  46. Yoo J, SS K. Probiotics and prebiotics: present status and future perspectives on metabolic disorders. *Nutrients* [Internet]. 2016;8:173. Available from: <https://www.ncbi.nlm.nih.gov/pmc/articles/PMC4808900/>
  47. Zhou T, Che D, Lan Y, Fang Z, Xie J, Gong H. Mesenchymal marker expression is elevated in Müller cells exposed to high glucose and in animal models of diabetic retinopathy. *Oncotarget* [Internet]. 2017;8:4582–94. Available from: <https://www.ncbi.nlm.nih.gov/pmc/articles/PMC5354856/>
  48. Jiao C, Spee C, Mullins RF, Hinton DR. APOPTOSIS AND ANGIOFIBROSIS IN DIABETIC TRACTIONAL MEMBRANES AFTER VASCULAR ENDOTHELIAL GROWTH FACTOR INHIBITION Results of a Prospective Trial . Report No . 2. Retina [Internet]. 2019;39:265–73. Available from: <https://insights.ovid.com/pubmed?pmid=29190236>
  49. Na L, Xiao-Rong L, Jia-qin Y. Effects of bone-marrow mesenchymal stem cells transplanted into vitreous cavity of rat injured by ischemia/reperfusion. *Graefe's Arch Clin Exp Ophthalmol*. 2009;247:503–14.
  50. Rajashekhar G. Mesenchymal stem cells: new players in retinopathy therapy. *Front Endocrinol (Lausanne)* [Internet]. Switzerland; 2014;24:59. Available from: <https://www.ncbi.nlm.nih.gov/pmc/articles/PMC4006021/>
  51. Safwat A, Sabry D, Ragiaie A, Amer E, Mahmoud RH, Shamardan RM. Adipose mesenchymal stem cells-derived exosomes attenuate retina degeneration of streptozotocin-induced diabetes in rabbits. *J Circ biomarkers* [Internet]. United States; 2018;7:1–10. Available from: <https://www.ncbi.nlm.nih.gov/pmc/articles/PMC6207964/>
  52. Kramerov AA, Ljubimov AV. Stem cell therapies in the treatment of diabetic retinopathy and keratopathy. *Exp Biol Med (Maywood)* [Internet]. England; 2016;241:559–68. Available from: <https://www.ncbi.nlm.nih.gov/pmc/articles/PMC4950324/>
  53. Zhang Y, Wang W. Effects of bone marrow mesenchymal stem cell transplantation on light-damaged retina. *Invest Ophthalmol Vis Sci* [Internet]. United States; 2010;51:3742–8. Available from: <https://iovs.arvojournals.org/article.aspx?articleid=2127062>
  54. Ezquer M, Urzua CA, Montecino S, Leal K, Conget P, Ezquer F. Intravitreal administration of multipotent mesenchymal stromal cells triggers a cytoprotective microenvironment in the retina of diabetic mice. *Stem Cell Res Ther* [Internet]. England; 2016;7:42. Available from: <https://stemcellres.biomedcentral.com/articles/10.1186/s13287-016-0299-y>
  55. da Silva-Junior AJ, Mesentier-Louro LA, Nascimento-Dos-Santos G, Teixeira-Pinheiro LC, Vasques JF, Chimeli-Ormonde L, et al. Human mesenchymal stem cell therapy promotes retinal ganglion cell survival and target reconnection after optic nerve crush in adult rats. *Stem Cell Res Ther*. 2021;12(1):69. <https://doi.org/10.1186/s13287-020-02130-7>.
  56. Mathew B, Ravindran S, Liu X, Torres L, Chennakesavalu M, Huang C, et al. Mesenchymal stem cell-derived extracellular vesicles and retinal ischemia- reperfusion. *Biomaterials* [Internet]. Elsevier; 2019;197:146–60. Available from: <https://doi.org/10.1016/j.biomaterials.2019.01.016>

**Publisher's Note** Springer Nature remains neutral with regard to jurisdictional claims in published maps and institutional affiliations.

Springer Nature or its licensor (e.g. a society or other partner) holds exclusive rights to this article under a publishing agreement with the author(s) or other rightsholder(s); author self-archiving of the accepted manuscript version of this article is solely governed by the terms of such publishing agreement and applicable law.